Eur. Phys. J. D **28**, 181–185 (2004)
DOI: 10.1140/epjd/e2003-00311-6

THE EUROPEAN PHYSICAL JOURNAL D

Families of matter-waves in two-component Bose-Einstein condensates

P.G. Kevrekidis[1,a], H.E. Nistazakis[2], D.J. Frantzeskakis[2], B.A. Malomed[3], and R. Carretero-González[4]

[1] Department of Mathematics and Statistics, University of Massachusetts, Amherst MA 01003-4515, USA
[2] Department of Physics, University of Athens, Panepistimiopolis, Zografos, Athens 15784, Greece
[3] Department of Interdisciplinary Studies, Tel Aviv University, Tel Aviv 69978, Israel
[4] Nonlinear Dynamical Systems Group[b], Department of Mathematics and Statistics, San Diego State University, San Diego CA, 92182-7720, USA

Received 8 July 2003
Published online 16 December 2003 –

Abstract. We produce several families of solutions for two-component nonlinear Schrödinger/Gross-Pitaevskii equations. These include domain walls and the first example of an antidark or gray soliton in one component, bound to a bright or dark soliton in the other. Most of these solutions are linearly stable in their entire domain of existence. Some of them are relevant to nonlinear optics, and all to Bose-Einstein condensates (BECs). In the latter context, we demonstrate robustness of the structures in the presence of parabolic and periodic potentials (corresponding, respectively, to the magnetic trap and optical lattices in BECs).

PACS. 03.75.-b Matter waves – 52.35.Mw Nonlinear phenomena: waves, wave propagation, and other interactions (including parametric effects, mode coupling, ponderomotive effects, etc.)

The recent progress in experimental and theoretical studies of Bose-Einstein condensates (BECs) [1] has made matter-wave solitons physically relevant objects. One dimensional (1D) dark [2] and bright [3] solitons have been observed in experiments, and possibilities for the observation of their multidimensional counterparts were predicted [4]. Further study of matter-wave solitons is a subject of profound interest, not only from a theoretical perspective, but also for applications, as there are possibilities to coherently manipulate such robust structures in matter-wave devices, e.g., atom chips, which are analogs of the existing optical ones [5]. On the other hand, many results obtained for optical solitons as fundamental nonlinear excitations in optical fibers and waveguides (see, e.g., recent reviews [6,7]) suggest the possibility to search for similar effects in BECs.

A class of physically important generalizations of the nonlinear Schrödinger (NLS) equation for optical media, or its BEC counterpart, the Gross-Pitaevskii equation (GP), is based on their multi-component versions. In particular, the theoretical work has already gone into studying ground-state solutions [8,9] and small-amplitude excitations [10] of the order parameters in multi-component BECs. Additionally, the structure of binary BECs [11], including the formation of domain walls in the case of immiscible species, has also been studied [11,12]; 1D bound dark-dark [13] and dark-bright [14] soliton complexes, as well as spatially periodic states [15], were predicted too. Experimental results have been reported for mixtures of different spin states of ^{87}Rb [16] and mixed condensates [17]. Efforts were also made to create two-component BECs with different atomic species, such as ^{41}K–^{87}Rb [18] and ^{7}Li–^{133}Cs [19].

In this work, we report novel solitons in the context of coupled two-component GP equations. These solutions correspond to new families of solitons even for the NLS equations per se, hence they are also interesting as nonlinear waves in their own right. We start by demonstrating their existence in the context of two coupled NLS equations. Some of them are relevant as new solitons in nonlinear-optical models as well. We also demonstrate that all the solutions proposed herein persist in the presence of the magnetic trap and optical lattice (OL), i.e., parabolic and sinusoidal potentials [20], which are important ingredients of experimental BEC setups.

Assuming that the nonlinear interactions are weak relative to the confinement in the transverse dimensions, the transverse size of the condensate is much smaller than its lengths. In this case, the BEC is a "cigar-shaped" one, and the GP equations take an effectively 1D form [21]:

$$i\frac{\partial u_j}{\partial t} = -\frac{m_1}{m_j}\frac{\partial^2 u_j}{\partial x^2} + \sum_{k=1}^{2} a_{jk}|u_k|^2 u_j + V_j(x)u_j, \quad (j=1,2) \tag{1}$$

[a] e-mail: kevrekid@math.umass.edu
[b] http://nlds.sdsu.edu/

where $u_j(x,t)$ are the mean-field wave functions of the two species, t and x are, respectively, measured in units of $2/\omega_{1\perp}$ and the transverse harmonic-oscillator length $a_{1\perp} \equiv \sqrt{\hbar/(m_1\omega_1)}$ (m_j and $\omega_{j\perp}$ are the mass and transverse confining frequency of each species), while $\hbar\omega_{1\perp}/2$ is the energy unit. The coefficients a_{jk} in equation (1), related to the three scattering lengths α_{jk} (note that $\alpha_{12} = \alpha_{21}$) through $a_{jk} = 4\pi m_1(\alpha_{jk}/a_{1\perp})(m_j + m_k)/(m_j m_k)$, account for collisions between atoms belonging to the same (a_{jj}) and different (a_{jk}, $j \neq k$) species; they are counterparts of the, respectively, self-phase and cross-phase modulation in nonlinear optics. While in optics only specific ratios of the nonlinear coefficients are relevant (such as $a_{ij}/a_{ii} = 2$ or $a_{ij}/a_{ii} = 2/3$ [6]), in the BEC context the interactions are tunable [9,15], especially because they can be modified by means of the Feshbach resonance (i.e., by magnetic field affecting the sign and magnitude of the scattering length of the interatomic collisions) [22]. The Feshbach resonance allows one to switch between attractive and repulsive interaction [23], and even to switch it periodically in time, by means of an ac magnetic field, which allows one to create a self-confined 2D BEC without the magnetic trap [24].

In this work, we consider the case with $m_1 = m_2 \equiv m$ and $a_{11} = a_{22}$, which corresponds to the most experimentally feasible mixture of two different hyperfine states of the same atom species, or, approximately, to different isotopes of the same alkali metal, trapped in the potential including the magnetic trapping and OL components:

$$V_1(x) = V_2(x) \equiv V(x) = \left(\Omega^2/2\right) x^2 + V_0 \sin^2(kx+\phi). \quad (2)$$

In equation (2), $\Omega^2 \equiv 2\omega_x^2/\omega_\perp^2$ ($\omega_{1x} = \omega_{2x} \equiv \omega_x$ are the confining frequencies in the axial direction) and V_0 (measured in units of the recoil energy [20]) set the respective potential strengths, k is the wavenumber of the interference pattern of the laser beams forming the OL, and ϕ is an adjustable phase parameter ($\phi \in \{0, \pi/2\}$). To estimate physical parameters, we resort to a mixture of two different spin states of ^{87}Rb, confined in a trap with the transverse frequency $\omega_{1\perp} = 183$ rad/s, which implies that the length and time units are 2 μm and 5.46 ms, respectively.

We consider a rather general case, in which the interatomic interactions in the first species are repulsive [therefore, we will use the normalization $a_{11} \equiv +1$ in Eqs. (1)], while in the other species they may be either attractive or repulsive. As concerns the interactions between the different species, they are, typically, repulsive. Nevertheless, in the case of two different spin states of the same atom species, the Feshbach resonance between such states is possible too (experimental studies of the Feshbach resonance in this case are currently in progress [25]), therefore attractive inter-species interactions may be relevant, and this case is also considered below. The solutions reported herein, and their existence and stability regimes are summarized in Table 1.

In most cases the existence and stability of the solution families is investigated numerically. The numerical method was implemented as follows: we first seek stationary solutions by means of Newton iterations which are applied to the steady-state equations $\mu u_j = -u_{j,xx} + \sum_{k=1}^{2} a_{jk}|u_k|^2 u_j + V(x)u_j$ (μ is the chemical potential). Subsequently, we perform the linear-stability analysis of the obtained soliton solutions $u_j^{(0)}(x)$, setting the perturbed solution to be

$$u_j = e^{-i\mu t}\left[u_j^{(0)}(x) + \epsilon\left(b_j e^{-i\omega t} + c_j e^{i\omega^* t}\right)\right],$$

where $\omega \equiv \omega_r + i\omega_i$ is a (generally, complex) perturbation eigenfrequency. Then, the ensuing linear stability problem [26] is solved for the eigenfrequencies and eigenfunctions $\{b_j, c_j^*\}$. Whenever the solution is unstable, we also examine its evolution in direct simulations of the full equations (1), using a fourth-order Runge-Kutta time integrator with the time step $dt = 0.005$ (27.3 μs in physical units). To initiate the instability development, a uniformly distributed random perturbation of amplitude $\sim 10^{-4}$ was typically added to an unstable solution.

Table 1. Existence and stability of structures in the binary BEC. In the "existence" column, $+/-$ indicates the repulsive/attractive character of the respective inter-atomic interaction which is necessary for the solution to exist. The "stability" column indicates the sign of the coefficient a_{22} (we normalize $a_{11} \equiv +1$, and set $a_{22} = \pm 1$) and an interval of the values of a_{12} for which the solution is stable.

Types of solitons	*Existence*		*Stability*	
	a_{22}	a_{12}	a_{22}	a_{12}
Domain wall	$+$	$+$	$+1$	> 1
Dark-antidark	$+$	$+$	$+1$	$(0, 0.7]$
Dark-gray	$+$	$-$	$+1$	$[-0.83, 0)$
Bright-antidark	$-$	$-$	-1	$(-1, 0)$
Bright-gray	$-$	$+$	-1	> 0

We now examine in detail the solutions shown in Table 1. First, in the absence of the external potential, a family of domain walls can be found in an exact form for the special case, $a_{12} = 3a_{11} = 3a_{22}$:

$$u_j(x,t) = Ae^{-i\mu t}\left[1 + (-1)^j \tanh(\eta x)\right], \quad (3)$$

where the chemical potential is $\mu = 4a_{12}A^2$, and $\eta^2 = 2a_{12}A^2$ (they follow the pattern of domain-wall solutions found long ago in the context of coupled Ginzburg-Landau equations [27]). These solutions exist only if $a_{12} > 0$ and $\mu > 0$. Similar patterns were found in reference [12] and other related structures were also predicted to occur in higher dimensions [28].

We have confirmed the existence and stability of the domain walls by direct numerical simulations (not shown here), using numerical continuation to extend them to the case $a_{12} \neq 3a_{11}$, where the analytical solution is not available. We have thus found that the domain walls exist and are stable for values of a_{12} down to $a_{12} = 1$. The case $a_{12} = 2$ is relevant to nonlinear optics; stability of the domain wall family for this case was suggested by recent numerical results obtained for a similar discrete coupled-NLS model [29]. Here, we find that these solutions are robust as well for other values of a_{12}, and, as will be shown

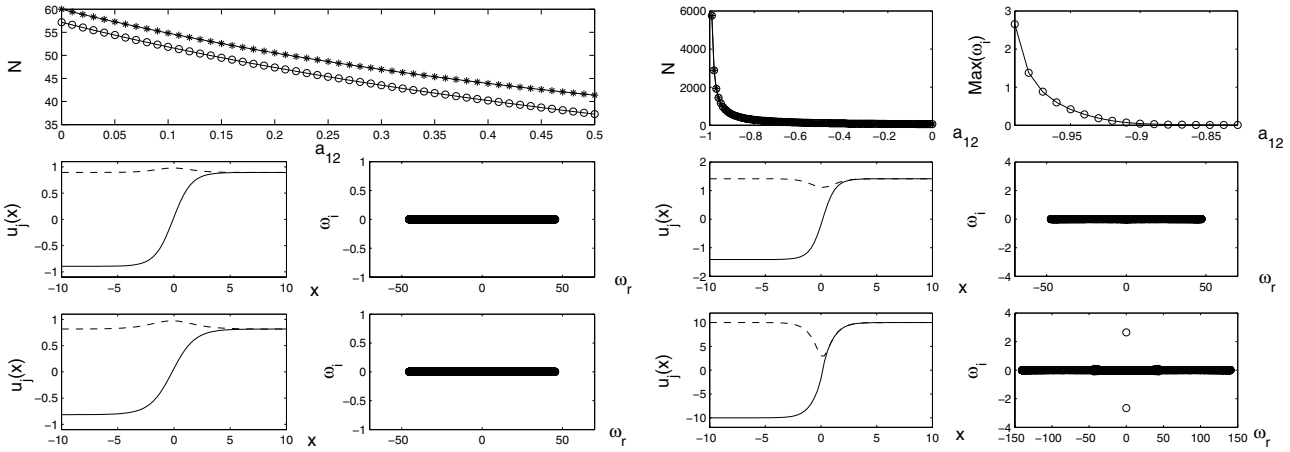

Fig. 1. Left: the top panel shows the number of atoms (in normalized units) in each component (circles and stars) of the dark-antidark soliton. The middle and bottom left panels show the spatial profiles of this solution for $a_{12} = 0.2$ and $a_{12} = 0.5$, while the right panels show the respective spectral planes (ω_r, ω_i) of the corresponding eigenfrequencies, as found from the linearized equations ($\omega_i = 0$ implies linear stability). Right: the top panels show the number of atoms in each component of the dark-gray soliton and the instability growth versus a_{12}. The middle and bottom left panels show the spatial profiles of this solution for $a_{12} = -0.5$ and $a_{12} = -0.99$, while the right panels show the respective spectral planes.

below, also in the presence of the external potential in equation (2).

Proceeding to the other solutions in Table 1, we first note that, upon fixing $a_{11} \equiv +1$, we set $a_{22} = \pm 1$ for the repulsive and attractive interactions in the second species. Although setting $|a_{22}|$ to be 1 formally limits the generality of the results, it has been checked that taking $|a_{22}| \neq 1$ produces results similar to those displayed here.

Given that we have assumed the first component as being always self-repulsive, we look for solutions starting from the uncoupled limit ($a_{12} = 0$) by taking an initially uniform distribution in this component, $u_1 \equiv 1$. If the second component is also repulsive, we take a dark soliton as its initial configuration. If it is self-attractive, a bright soliton is initially set in it.

The case of the self-repulsion and dark soliton in the second component, with the inter-species coefficient being *repulsive* too, $a_{12} > 0$ gives rise to a stationary *antidark soliton* (i.e., a hump on top of a nonzero flat background) in the first component, see the left panel in Figure 1. It is easy to understand this structure, as the atoms in the first component, being repelled by the matter in the second one, concentrate in an effective potential well generated by the dark soliton (void) in it. Antidark solitons are well-known to occur when higher-order effects (such as third-order dispersion) or a saturable nonlinearity are present in the single-component NLS equations, which is possible in optics [7]. In that case, the antidark soliton is usually described by a KdV-type asymptotic equation (for the elevation on top of the flat background), and is not stationary, running at the respective velocity of sound [7]. The two-species soliton with the antidark component, presented here, is the first example of a stationary antidark soliton, that we are aware of, in a model without higher-order nonlinearities and dispersions. It is also the *first prediction* of antidark solitons in BECs, which suggests that an experimental verification would be of particular interest.

If, on the contrary, the interaction between the two self-repelling species is *attractive* ($a_{12} < 0$; right panel in Fig. 1), then the void (dark soliton) in the second component effectively repels the matter in the first one, and thus generates a dip, i.e. a *gray soliton* in it (for a detailed description, see Ref. [7]). Such solitons exist in the regular NLS equation, but there (as well as in other instances of their presence that we are aware of) they travel at a nonzero speed (the faster the shallower the dip is), while here the gray solitons are stationary.

The bound dark-antidark two-component states persist for $0 < a_{12} \leq 0.7$, while the dark-gray bound-state branch continues down to $a_{12} = -1$, getting appreciably unstable in the region $-1 < a_{12} < -0.83$. In the latter case, the time evolution (not shown here) leads to formation of *moving* dark-gray soliton complexes.

Similar results were obtained for the last two branches of the new solutions: if the second component is now self-attractive, then the attractive interaction between the BEC species ($a_{22} = -1, a_{12} < 0$; see left panel in Fig. 2) gives rise to *bright-antidark solitons* (whose existence is explained by the fact that the bright soliton attracts matter in the other component). Such a type of two-component solitons was predicted in optics [30], but there it cannot exist without the third-order dispersion. In our case, this solution branch terminates at $a_{12} = -1$, since both states become completely flat.

Lastly, if the bright soliton repels matter in the other component, it naturally induces a dip in it, thus generating a *bright-gray soliton* in the case of $a_{22} = -1, a_{12} > 0$ (right panel Fig. 2). It is noteworthy that this bright-gray branch is extremely robust; we were able to follow such stable solutions down to $a_{12} = -3$.

We have also examined these novel solutions in the presence of the OL [i.e., for $V_0 \neq 0$, $\Omega = 0$ in Eq. (2)].

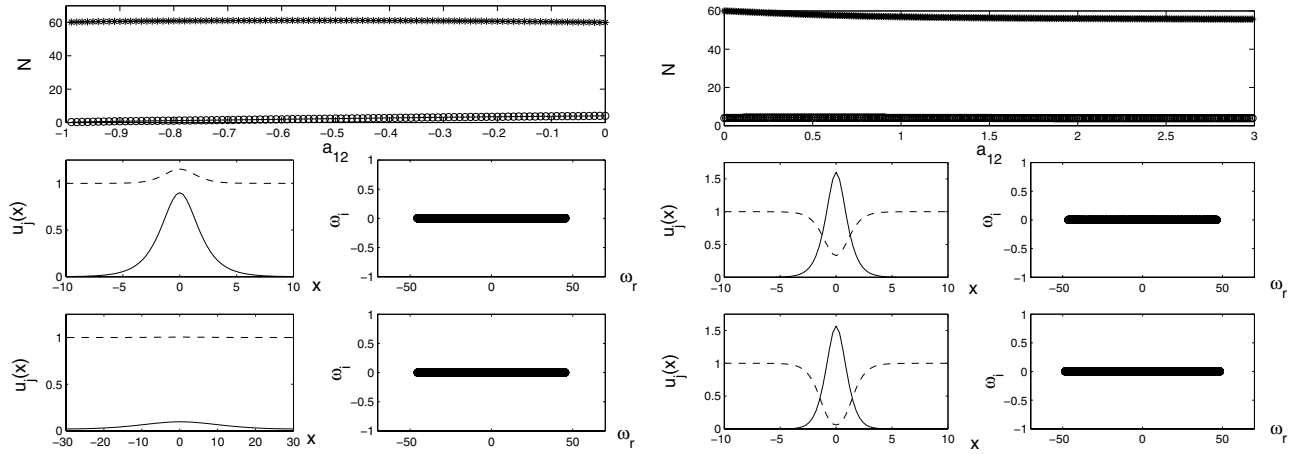

Fig. 2. Left: same as Figure 1 but for the bright-antidark solitons. The middle and bottom panels are for $a_{12} = -0.5$ and $a_{12} = -0.99$, respectively. Right: the branch of coupled bright-gray solitons. The middle and bottom panels are for $a_{12} = 0.2$ and 0.5, respectively.

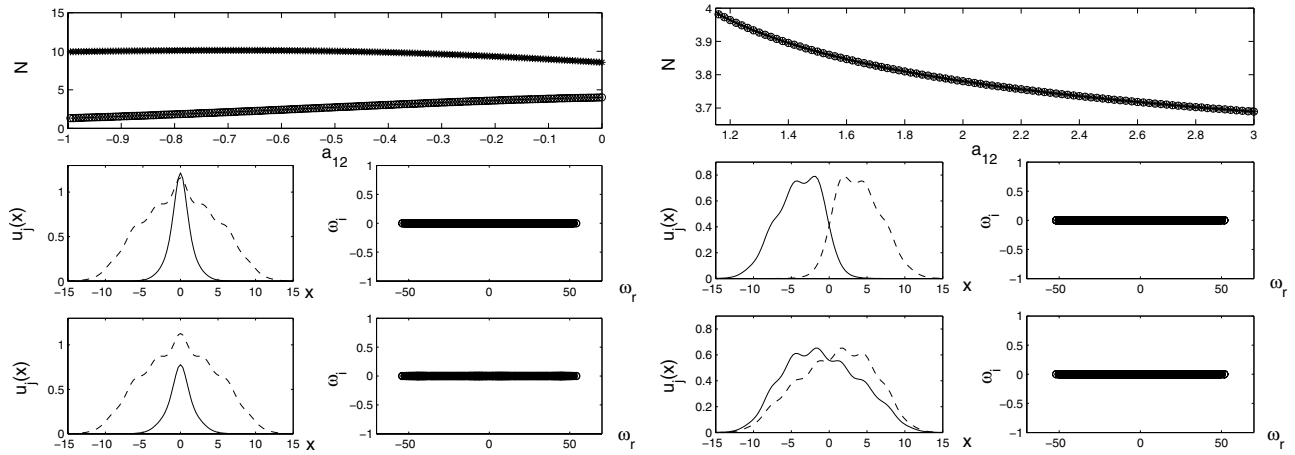

Fig. 3. Left: the bright-antidark branch (the middle and bottom panel are for $a_{12} = -0.5$ and -1, respectively) in the presence of the potential $V(x) = 0.01x^2 + 0.5\sin^2(x)$, see equation (2). Right: the same for the domain-wall solutions (the middle and bottom panels are for $a_{12} = 3$ and 2, respectively).

We have found them to be typically stable when $\phi = 0$, and unstable when $\phi = \pi/2$ (as might be expected, since the solution is then placed, respectively, at a minimum and maximum of the potential). However, there are exceptions to this rule. For instance, dark-antidark bound solitons for $a_{12} = 0.5$ are unstable at $\phi = 0$, in intervals $0.04 \leq V_0 \leq 0.055$ and $0.09 \leq V_0 \leq 0.29$. This oscillatory instability, involving a quartet of eigenvalues, will be examined in detail elsewhere.

We have also identified all the solution branches in the presence of the magnetic trap, as well as in the case when both the magnetic trap and the OL are present. The branches are extremely robust in the presence of the magnetic trap. In particular, Figure 3 shows the branches for the bright-antidark bound state (left panel) and domain walls (right panel), which are *always stable* in the presence of the combined potential with $\Omega^2 = 0.02$ and $V_0 = 0.5$. In particular, for a mixture of two different spin states of ^{87}Rb, the confining frequencies corresponding to this value of Ω are $\omega_x = 18.3$ rad/s and $\omega_{1\perp} = 183$ rad/s in the transverse and axial directions, respectively. Then, the four cases shown in Figure 3 correspond to the mixture containing, in the first and second species, 2×10^4 and 6×10^3 atoms ($a_{12} = -0.5$), 2×10^4 and 3×10^3 atoms ($a_{12} = -1$), 7.4×10^3 in each component ($a_{12} = 3$), and, finally, 7.6×10^3 atoms in each component ($a_{12} = 2$), respectively.

Finally, we notice that the increasing interaction between the components can play a stabilizing role for solutions that are unstable in the OL with $\phi = \pi/2$ (Fig. 4). The dark-antidark coupled state serves as an example, being unstable for $0 < a_{12} < 0.4$ and stable for $a_{12} > 0.4$ (left panel). The instability evolution is shown in the right panel for $a_{12} = 0.2$: the dark soliton becomes mobile and starts to oscillate in the combined potential. For the physical example mentioned above, the numbers of atoms in the two components corresponding to the latter case are 10^4 and 1.6×10^4, respectively.

In conclusion, we have presented a number of novel families of composite solutions in the generic two-species

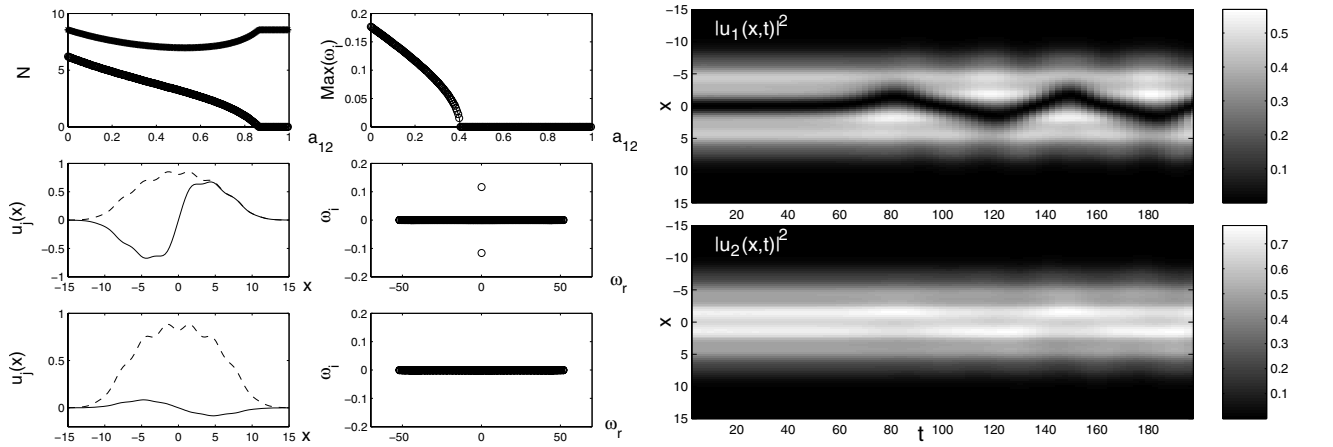

Fig. 4. Left: the dark-antidark solution branch for $\phi = \pi/2$. The branch is unstable at $a_{12} < 0.4$ (an example is displayed for $a_{12} = 0.2$, in the middle panel), and then it gets stabilized (see an example for $a_{12} = 0.86$ in the bottom panel). Right: time evolution of the unstable soliton in the case $a_{12} = 0.2$ with a random perturbation of an amplitude $\sim 10^{-4}$ added to the initial condition. The instability leads to an oscillating dark soliton. The time unit is 5.46 ms, hence the onset of instability occurs at ≈ 0.33 s.

BEC model. In particular, the first possibility to create an antidark soliton in BECs is predicted. In most cases, the compound solitons and domain walls are very robust, keeping the stability in the presence of the parabolic and periodic potentials. In some cases, the new solutions are relevant to optical models as well. It would be of interest to look for such states experimentally.

We appreciate a valuable discussion with D.S. Hall. This work was supported by a UMass FRG, NSF-DMS-0204585 and the Eppley Foundation (PGK), the Special Research Account of the University of Athens (HEN, DJF), the Binational (US-Israel) Science Foundation under grant No. 1999459 (BAM) and the San Diego State University Foundation (RCG).

References

1. F. Dalfovo et al., Rev. Mod. Phys. **71**, 463 (1999)
2. S. Burger et al., Phys. Rev. Lett. **83**, 5198 (1999); J. Denschlag et al., Science **287**, 97 (2000); B.P. Anderson et al., Phys. Rev. Lett. **86**, 2926 (2001)
3. K.E. Strecker et al., Nature **417**, 150 (2002); L. Khaykovich et al., Science **296**, 1290 (2002)
4. B.B. Baizakov, V.V. Konotop, M. Salerno, J. Phys. B **35**, 5105 (2002); E.A. Ostrovskaya, Y.S. Kivshar, Phys. Rev. Lett. **90**, 160407 (2003); B.B. Baizakov, B.A. Malomed, M. Salerno, Europhys. Lett. **63**, 642 (2003)
5. R. Folman, J. Schmiedmayer, Nature **413**, 466 (2001); R. Folman et al., Adv. Atom. Mol. Opt. Phys. **48**, 263 (2002)
6. B.A. Malomed, Progr. Opt. **43**, 71 (2002); A.V. Buryak et al., Phys. Rep. **370**, 63 (2002)
7. Yu.S. Kivshar, B. Luther-Davies, Phys. Rep. **298**, 81 (1998)
8. T.-L. Ho, V.B. Shenoy, Phys. Rev. Lett. **77**, 3276 (1996); H. Pu, N.P. Bigelow, Phys. Rev. Lett. **80**, 1130 (1998)
9. B.D. Esry et al., Phys. Rev. Lett. **78**, 3594 (1997)
10. Th. Busch et al., Phys. Rev. A **56**, 2978 (1997); R. Graham, D. Walls, Phys. Rev. A **57**, 484 (1998); H. Pu, N.P. Bigelow, Phys. Rev. Lett. **80**, 1134 (1998); B.D. Esry, C.H. Greene, Phys. Rev. A **57**, 1265 (1998)
11. M. Trippenbach et al., J. Phys. B **33**, 4017 (2000)
12. S. Coen, M. Haelterman, Phys. Rev. Lett. **87**, 140401 (2001)
13. P. Öhberg, L. Santos, Phys. Rev. Lett. **86**, 2918 (2001)
14. Th. Busch, J.R. Anglin, Phys. Rev. Lett. **87**, 010401 (2001)
15. B. Deconinck et al., J. Phys. A **36**, 5431 (2003)
16. C.J. Myatt et al., Phys. Rev. Lett. **78**, 586 (1997)
17. D.S. Hall et al., Phys. Rev. Lett. **81**, 1539 (1998); D.M. Stamper-Kurn et al., Phys. Rev. Lett. **80**, 2027 (1998)
18. G. Modugno et al., Science **294**, 1320 (2001)
19. M. Mudrich et al., Phys. Rev. Lett. **88**, 253001 (2002)
20. See e.g., F.S. Cataliotti et al., Science **293**, 843 (2001); A. Trombettoni, A. Smerzi, Phys. Rev. Lett. **86**, 2353 (2001); M. Greiner et al., Appl. Phys. B **73**, 769 (2001)
21. V.M. Pérez-García et al., Phys. Rev. A **57**, 3837 (1998); L. Salasnich et al., Phys. Rev. A **65**, 043614 (2002); Y.B. Band, I. Towers, B.A. Malomed, Phys. Rev. A **67**, 023602 (2003)
22. S. Inouye et al., Nature **392**, 151 (1998); E.A. Donley et al., Nature **412**, 295 (2001)
23. P.G. Kevrekidis et al., Phys. Rev. Lett. **90**, 230401 (2003)
24. F.Kh. Abdullaev et al., Phys. Rev. A **67**, 013605 (2003); H. Saito, M. Ueda, Phys. Rev. Lett. **90**, 040403 (2003)
25. D.S. Hall, private communication
26. C. Sulem, P.L. Sulem, *The Nonlinear Schrödinger Equation* (Springer-Verlag, New York, 1999) [see particularly Sect. 4.1 and references therein]. The resulting linearization problem is a matrix eigenvalue problem (in the finite difference setting) whose solution is provided by standard numerical linear algebra packages
27. B.A. Malomed, A.A. Nepomnyashchy, M.I. Tribelsky, Phys. Rev. A **42**, 7244 (1990)
28. E. Timmermans, Phys. Rev. Lett. **81**, 5718 (1998); B.D. Esry, C.H. Greene, Phys. Rev. A **59**, 1457 (1999); D.T. Son, M.A. Stephanov, Phys. Rev. A **65**, 063621 (2002)
29. P.G. Kevrekidis et al., Phys. Rev. E **67**, 036614 (2003)
30. D.J. Frantzeskakis, Phys. Lett. A **285**, 363 (2001)